GEOPHYSICAL RESEARCH LETTERS, VOL. 28, NO. 7, PAGES 1171-1174, APRIL 1, 2001

A possible correlation between satellite-derived cloud and aerosol microphysical parameters

Teruyuki Nakajima
Center for Climate System Research, The University of Tokyo, Japan

Akiko Higurashi
National Institute for Environmental Studies, Japan

Kazuaki Kawamoto
Virginia Polytechnic Institute and State University, Virginia

Joyce E. Penner
Department of Atmosphere, Oceanic and Space Sciences, University of Michigan

Abstract. The column aerosol particle number and low cloud microphysical parameters derived from AVHRR remote sensing are compared over ocean for four months in 1990. There is a positive correlation between cloud optical thickness and aerosol number concentration, whereas the effective particle radius has a negative correlation with aerosol number. The cloud liquid water path (LWP), on the other hand, tends to be constant with no large dependence on aerosol number. This result contrasts with results from recent model simulations which imply that there is a strong positive feedback between LWP and aerosol number concentration. Estimates for indirect forcing over oceans derived from the satellite data/model comparison range from -0.7 to -1.7 Wm^{-2}.

1. Introduction

Anthropogenic aerosols can significantly affect the earth s climate [*Twomey et al.*, 1984; *Charlson et al.*, 1992]. Yet the assessed magnitude of the radiative forcing due to anthropogenic aerosols is quite uncertain because the mechanisms which determine the forcing are complex [*IPCC95*, 1996]. This is especially true for the indirect effect of aerosols which occurs because aerosols act as cloud condensation nuclei (CCN). Two kinds of indirect effects have been recognized. The first effect is a change in the cloud radiative properties due to cloud particle radius reduction, and the second effect is a change in cloud drop number concentration which further produces change in LWP, cloud amount, and radiative properties. The evaluated magnitude of the first indirect effect ranges from –2 W/m^2 to 0 W/m^2 [*Charlson et al.*, 1992; *IPCC95*, 1996; *Hansen et al.*, 1998]. Climate models have shown that the second indirect effect can more than double the forcing calculated for the first indirect effect [e.g. *Jones et al.*, 1994; *Chuang et al.*, 1997; *Rotstayn*, 1999; *Lohmann et al.*, 1999; *Kiehl et al.*, 2000].

There have been several observations of the indirect effect from satellite for contamination of clean marine air by ship effluence [*Coakley et al*, 1987; *Radke et al.*, 1989] and city pollution [*Rosenfeld*, 2000]. The global retrieval by *Han et al.* [1994] shows a noticeable decrease in the effective radius of low clouds around land regions compared to that in ocean regions that is highly suggestive of an indirect effect. An important unresolved issue, however, is whether or not the liquid water path increases when aerosol concentrations increase. A significant increase in LWP has been observed by several researchers [*Radke et al.*, 1989; *Nakajima and Nakajima*, 1995], but there are other observations that suggest this effect is insignificant [*Platnick et al.*, 2000]. *Wetzel and Stowe* [1999] have compared the aerosol optical thickness and cloud properties, but their forcing estimates have a large uncertainty because they could not estimate aerosol number.

In this paper, we present a simultaneous analysis of cloud and aerosol parameters from a newly developed algorithms for AVHRR remote sensing.

2. Remote sensing of cloud and aerosol fields

There are several pioneering studies for deriving the global distribution of aerosol parameters [*Husar et al.*, 1997; *Nakajima and Higurashi*, 1998; *Goloub et al.*, 1999]. In this study we adopt the AVHRR algorithm of *Higurashi and Nakajima* [1999] to derive the optical thickness τ_a and ngstr m exponent α. The optical thickness dependence on wavelength of light λ is fitted to

$$\tau_\lambda = \tau_a (\lambda/\lambda_0)^{-\alpha}. \quad (1)$$

and the reference wavelength is set as λ_0 = 0.5 m. The ngstr m exponent can be related to the shape of the size distribution and hence can be used as a size index. This information is extremely important for evaluating the column number of aerosol particles and CCN. The algorithm retrieves the peak volume values V_1 and V_2 of a bimodal log-normal size distribution from red and near-infrared channels of a sensor, such that,

$$\frac{dV}{d\ln r} = \sum_{n=1}^{2} \frac{V_n}{\sqrt{2\pi}\sigma_n} \exp[-\frac{1}{2}(\frac{\ln r - \ln r_n}{\sigma_n})^2], \quad (2)$$

Paper number 2000GL012186
0094-8276/01/2000GL012186$05.00

where the mode radii and log-dispersions $\{r_n, \sigma_n | n=1,2\}$ are constant during the inversion with r_1=0.17 μm, r_2= 3.44 μm, σ_1= 0.26 and σ_2= 1.01. The retrieved V_1 and V_2 are further used for calculating the ngstr m parameters τ_a and α. The column aerosol number N_a is approximately given from Eq. (2) as

$$N_a \approx \tau_a \alpha \frac{\sigma_1}{\sqrt{2\pi} r_1^2} \exp\{4\sigma_1^2 + \frac{1}{2\sigma_1^2}[\ln(\frac{1.4\lambda}{2\pi r_1}) + \sigma_1^2]^2\}. \quad (3)$$

The equation shows that N_a is proportional to the product of two observables of remote sensing $\tau_a\alpha$. More accurate formula can be derived from analyzing actual satellite-data as N_a = 4.57x10^8 $(\tau_a\alpha)^\gamma$ (particles/cm^2) with γ= 0.869 with relative error of 20% (see Fig. 1). The figure shows that use of τ_a alone will cause a large error in estimated N_a. The present algorithm can retrieve τ_a and α with errors less than 0.05 and 0.1, respectively [*Goloub et al.*, 1999; *Higurashi et al.*, 2000]. The error in the estimated number is then caused mostly from assumed values of r_1 and σ_1. This error can reach a factor of 10 if the assumed values of r_1 and σ_1 are incorrect. The characteristic values of r_1 and σ_1, however, are similar for continental and marine aerosols, so that the relative change in the anthropogenic aerosol number can be accurately calculated as $\Delta N_a/N_a$ ¯ $\Delta(\tau_a\alpha)^\gamma/(\tau_a\alpha.)^\gamma$.

In the present study, we use the global distribution of cloud optical thickness τ_c and effective particle radius r_e, obtained by analysis of channel 1, 3 and 4 of AVHRR with the algorithm of *Kawamoto et al.* [2000]. Errors in τ_c and r_e have been estimated as less than 15% [*Nakajima et al.*, 1991; *Nakajima ana Nakajima*, 1995; *Kawamoto et al.*, 2000], so that the column cloud particle number N_c (particles/cm^2) and *LWP* (=2$\rho r_e \tau_c$/3 with water density ρ) are accurately estimated from τ_c and r_e.

Figure 2 shows the annual mean global distributions of aerosol and cloud parameters thus obtained for 0.5¡x0.5¡latitude-longitude segment boxes by averaging four months (Jan., April, July, and Oct.) in 1990. A pixel for low level clouds are selected with a brokenness test and cloud top temperature > 273K. It is found that there is a correlation

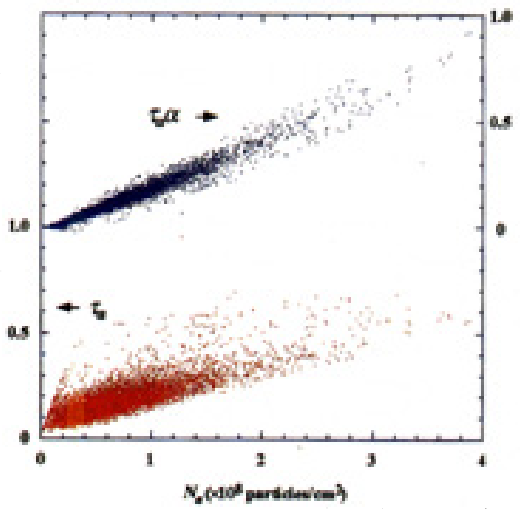

Figure 1. Scatter plots between N_a versus τ_a and $\tau_a\alpha$ for daily global retrieval results of AVHRR data in April 1990.

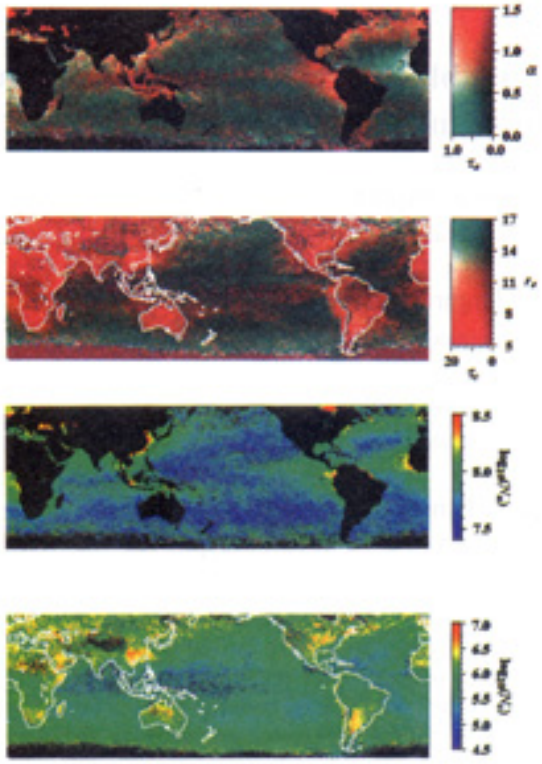

Figure 2. Global distribution of aerosol and cloud parameters. Four months average of τ_a, α, N_a (particles/cm^2), τ_c, r_e (m), and N_c (particles/cm^2). Color hue is assigned to α and r_e, and brightness to τ_a and τ_c for indicating features of small/large particles of aerosols and clouds, respectively.

between fine particle aerosol distributions characterized by large α and area for small r_e of low clouds in middle and high latitudes. Figure 3_compares values of N_a and N_c by assigning red and blue color, respectively. Regions adjacent to the east coasts of the continents and along the west coasts of South Africa, South America, and California are characterized by yellow color, indicating a positive correlation between N_a and N_c, as also pointed out by several investigators [*Coakley et al.*, 1987; *Han et al.*, 1994; *Nakajima and Nakajima*, 1995]. Most of the tropical region, on the other hand, is characterized by red color, i.e. small N_c in spite of large N_a. The main reason for this feature is that low clouds interacting with aerosols are not dominant in this region. It is also known that dust particles, one of dominant tropical aerosols, are not effective as CCN.

Aside from the moderately active region along the east coasts of continents and the inactive tropical regions (yellow and red colors, respectively), there are two other interesting regions. One is off the coast of California, where the greenish color shows large N_c in spite of small N_a, indicating that this region is an especially active region of cloud-aerosol interaction. This region is characterized by shallow stratocumulus clouds formed in the stable atmosphere of the subsiding Hadley cell over cold ocean currents. Ship trail clouds are frequently observed in this region [*Coakley et al.*, 1987; *Radke et al.*, 1989; *Platnick et al.*, 2000]. The other region of specific correlation is off the tropical west coast of Africa, where the yellow-colored area is mixed with red-colored area showing an active region mixed with an inactive region in Fig. 3. Satellite remote sensing and model calculation suggest that biomass burning aerosols as well as mineral dust aerosols are contributing to the atmospheric

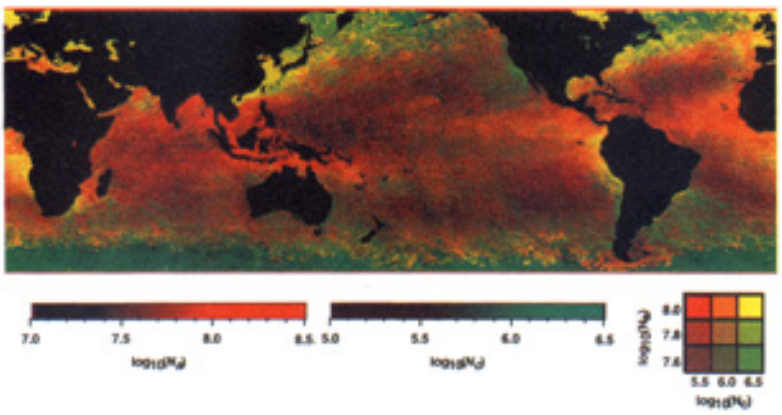

Figure 3. Global distribution of the correlation between N_a and N_c (particles/cm^2) as a four month average of 1990. Red color is assigned to N_a and green color to N_c. Bright yellow color shows both N_a and N_c are large, whereas bright red color shows N_c is small in spite of large N_a.

turbidity in this region [*Takemura et al.*, 2000]. Figure 4 shows global mean cloud parameters as a function of N_a for four seasons. In spite of a large variability, the figure shows a systematic negative correlation between r_e and N_a in a range of $10^{7.8} \dagger N_a \dagger 10^{8.5}$. The scatter plot between τ_c and N_a, on the other hand, shows a positive correlation in the same range of N_a. The tendency of the correlation from Fig. 4 can be summarized as

$$r_e \sim a_r + b_r \log_{10} N_a;\ \tau_a \sim a_\tau + b_\tau \log_{10} N_a;$$
$$\log_{10} N_c \sim a_N + b_N \log_{10} N_a \quad \text{for } 7.8 \dagger \log_{10} N_a \dagger 8.5, \qquad (4)$$

with a_r= 34.0–4.3 and b_r= -2.65–0.50; a_τ= -21.4–9.4 and b_τ= 3.30–1.32; a_N= 1.80–0.43 and b_N= 0.50–0.07. Indicated uncertainties were evaluated by results from various sampling methods of clear and cloudy pixels with changing average period as a day, three days, and one month. Small uncertainties in the regression coefficients suggest these characteristic correlations are a persistent signature of the indirect effect. On the other hand, LWP does not show a large trend. This behavior results from a cancellation of the negative and positive correlation of r_e and τ_c with N_a. Thus, the increase of LWP on a global scale is not as significant as that observed for ship trails off the California coast which was as large as 200% for a doubling of the aerosol concentration [*Radke et al.*, 1989].

The linear relationship between $\log_{10}N_a$ and $\log_{10}N_c$ in Fig. 4 is consistent with Twomey s formula [*Twomey*, 1977; *Kaufman et al.*, 1991] with a slope of b_N= 0.50. This log-slope relation is smaller than the range of 0.7 to 0.8 summarized by *Kaufman et al.*, [1991], but larger than proposed value of fitting the data of Martin et al. [1994]_(e.g. 0.26; c.f. *Jones et al.* [1994]). Figure 5 shows a scatter plot of the relationship between $\log_{10}N_c$ and $\log_{10}N_a$ from a model simulation using the Grantour/CCM1 model [*Penner et al.*, 1999]. The present simulation does not include_feedbacks to LWP from changes in droplet number. The figure shows that the Grantour/CCM1 model has a response for N_c that is positive throughout most of the range of $\log_{10}N_a$ with a_r= 39.9 and b_r= -3.85; a_N= 3.25 and b_N= 0.49. These values are comparable with those from the satellite results.

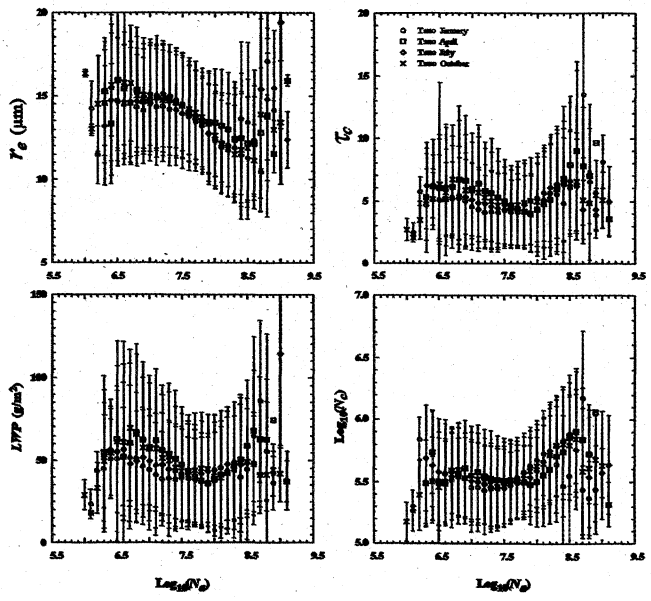

Figure 4. Scatter plots of the cloud parameters, r_e, τ_c, *LWP*, and N_c as a function of N_a. N_a and N_c are in particles/cm^2.

3. Discussion and conclusions

The correlation between satellite-derived aerosol number and cloud droplet number tells us that low clouds increase their shortwave reflectance with increasing cloud optical

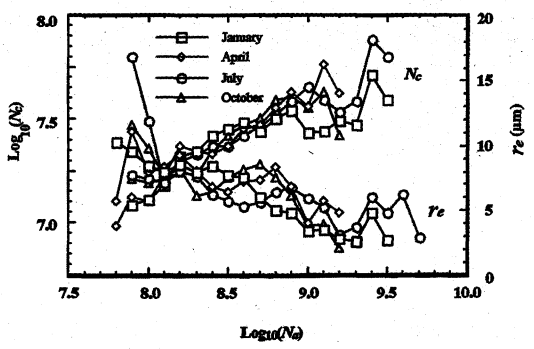

Figure 5. Scatter plots of N_c and r_e as a function of N_a determined from the model calculation. N_c and N_a are in particles/cm^2.

thickness when the aerosol number increases above a critical value around N_a=1.0$^{7.8}$. This increase in τ_c is caused mainly by the reduction in the effective cloud particle radius since on average there are insignificant changes in the LWP. The power law dependence of the cloud drop number concentration on aerosol number concentration is similar to that from the model calculation.

From the correlation presented by Eq. (4) and with a four-stream radiative transfer calculation, the perturbed shortwave cloud radiative forcing over ocean due to an aerosol increase is estimated as

$$\Delta crf = \Delta CRF/n \sim b_R \Delta \log_{10} N_a, \quad (5)$$

where n is the analyzed low level cloud amount over ocean. The slope is estimated as b_R = -30– 8 W/m^2. Using this relationship and normalizing by the ocean area results in a total estimated forcing over oceans of ΔCRF= -0.7– 0.2 Wm^{-2} if we assume n=0.38 and a 15% increase of anthropogenic aerosol particles [*Charlson et al.*, 1992]. Using the model estimated increase in aerosol number, e.g. 40% yields ΔCRF= -1.7– 0.4 Wm^{-2}. These values are comparable to model values from -1.69 Wm^{-2} for the model results from *Penner et al.* [1999] to -0.73 Wm^{-2} for the same model applied to the IPCC estimates for emissions [*Penner and Zhang*, 2000].

Acknowledgment. We are grateful to J. Tucker of NASA GSFC and R. Imasu of NIRE for providing AVHRR data. We extend gratitude to S. Katagiri, I. Ishii, and M. Sekiguchi for data analysis support. J. E. Penner thanks the ARM Program and the NASA Aerosol Program for support. C. Chuang provided useful discussions.

References

Charlson, R. J., S. E. Schwartz, J. M. Hales, R. D. Cess, J. A. Coakley, Jr., J. E. Hansen, D. J. Hofmann, Climate forcing by anthropogenic aerosols, *Science, 25*, 426-430, 1992.

Chuang, C. C., J. E. Penner, K. E. Taylor, A. S. Grossmann, and J. J. Walton, An assessment of the radiative effects of anthropogenic sulfate, *J. Geophys. Res, 102*, 3761-3778, 1997.

Coakley, J. A., Jr., R, L. Bernstein, and P. A. Durkee, Effect of ship-track effluents on cloud reflectivity, *Science, 237*, 1020-1022, 1987.

Goloub, P., D. Tanr , J. L. Deuz , M. Herman, A. Marchand, F. M. Br on, Validation of the first algorithm applied for deriving the aerosol properties over the ocean using the POLDER/ADEOS measurements, *IEEE Trans. Geosci. Remote Sensing*, 37, 1586-1596 , 1999.

Han, Q., W. B. Rossow, and A. A. Lacis, Near-global survey of effective droplet radii in liquid water clouds using ISCCP data, *J. Climate, 7*, 465-497, 1994.

Hansen, J. E., M. Sato, A. Lacis, R. Ruedy, I. Tegen, and E. Matthews, Climate forcings in the industrial era. *Proc. Natl. Acad. Sci. USA*, 95, 12753-12758, 1998.

Higurashi, A., and T. Nakajima, Development of a two channel aerosol retrieval algorithm on global scale using NOAA / AVHRR, *J. Atmos. Sci., 56*, 924-941, 1999.

Higurashi, A., T. Nakajima, B. N. Holben, A. Smirnov, R. Frouin, and B. Chatenet, A study of global aerosol optical climatology with two channel AVHRR remote sensing, *J. Climate*, 13, 2011-2027, 2000.

Husar, R. B., J. M. Prospero, and L. L. Stowe, Characterization of tropospheric aerosols over the oceans with the NOAA advanced very high resolution radiometer optical thickness operational product, *J. Geophys. Res., 102*, 16889-16910, 1997.

IPCC95, *Climate Change 1995, The science of climate change*, Edited by J. T. Houghton, L. G. Meira Filho, B. A. Callander, N. Harris, A. Kattenberg, and K. Maskell, Cambridge Univ. Press, 1996.

Jones, A., D. L. Roberts, and A. Slingo, A climate model study of indirect radiative forcing by anthropogenic sulphate aerosols, *Nature, 370*, 450-453. 1994.

Kaufman, Y. J., R. S. Fraser, and R. L. Mahoney, Fossil fuel and biomass burning effect on climate, *J. Climate, 4*, 578-588, 1991.

Kawamoto, K., T. Nakajima, and T. Y. Nakajima, A global determination of cloud microphysics with AVHRR remote sensing, *J. Climate*, 2000 (in press).

Kiehl, J. T., T. L. Schneider, P. J. Rasch, M. C. Barth, and J. Wong, Radiative forcing due to sulfate aerosols from simulations with the NCAR Community Climate Model (CCM3), *J. Geophys. Res., 105*, 1441-1458, 2000.

Lohmann, U., J. Feichter, C.C. Chuang, and J.E. Penner, Prediction of the number of cloud droplets in the ECHAM GCM, *J. Geophys. Res., 104*, 9169-9198, 1999.

Martin, G.M., D,W. Johnson, and A. Spice, The measurement and parameterization of effective radius of droplets in warm stratocumulus clouds, *J. Atmos. Sci., 51*, 1823-1842, 1994.

Nakajima, T., M. D. King, J. D. Spinhirne, and L. F. Radke, Determination of the optical thickness and effective radius of clouds from reflected solar radiation measurements. Part II: Marine Stratocumulus Observations, *J. Atmos. Sci., 48*, 728-750, 1991.

Nakajima, T. Y., and T. Nakajima, Wide-area determination of cloud microphysical properties from NOAA AVHRR measurements for FIRE and ASTEX regions, *J. Atmos. Sci., 52*, 4043-4059, 1995.

Nakajima, T., and A. Higurashi, A use of two-channel radiances for an aerosol characterization from space, *Geophys. Res. Lett., 25*, 3815-3818, 1998.

Penner, J. E., Chuang, C. C., and K. Grant, Climate change and radiative forcing by anthropogenic aerosols: Research findings during the last 5 years, *La Jolla International School of Science*, submitted, The Institute for Advanced Physics Studies, La Jolla, CA 92038-2946, March 29-30, 1999.

Penner, J. E., and Y. Zhang, Projections of climate forcing by sulfate, organic aerosols, dust, and sea salt: Results from the IPCC model intercomparison workshop, *Proc. the 11th Symposium on Global Change Studies*, 9-14 *January 2000, Long Beach, CA, American Meteorological Society, Boston, MA, p. 4 - 10*, 2000.

Platnick, S., P. A. Durkee, K. Nielsen, J. P. Taylor, S-C. Tsay, M. D. King, R. J. Ferek, P. V. Hobbs, and J. W. Rottman, The role of background cloud microphysics in the radiative formation of ship tracks, *J. Atmos. Sci., 57*, 2607-2624, 2000.

Radke, L. F., J. A. Coakley, Jr., and M. D. King, Direct and remote sensing observations of the effects of ships on clouds, *Science, 246*, 1146-1149, 1989.Rosenfeld, D., Suppression of rain and snow by urban and industrial air pollution. *Science*, 287, 1793-1796, 2000.

Rotstayn, L. D., Indirect forcing by anthropogenic aerosols: A global climate model calculation of the effective-radius and cloud-lifetime effect, *J. Geophys. Res., 102*, 9369-9380, 1999.

Takemura, T., H. Okamoto, Y. Maruyama, A. Numaguti, A. Higurashi, and T. Nakajima, Global three-dimensional simulation of aerosol optical thickness distribution of various origins. *J. Geophys. Res., 105*, 17853-17873, 2000.

Twomey, S., Atmospheric aerosols, 302pp, Elsevier Scientific Publ. Co., 1977.

Twomey, S., M. Piepgrass and T. L. Wolfe, An assessment of the impact of pollution on global cloud albedo. *Tellus, 36B*, 356-366, 1984.

Wetzel, M. A., and L. L. Stowe, Satellite-observed patterns in stratus microphysics, aerosol optical thickness, and shortwave radiative forcing, *J. Geophys. Res., 104*, 31287-31299, 1999.

T. Nakajima, Center for Climate System Research, The University of Tokyo, 4-6-1 Komaba, Meguro-ku, Tokyo, 153-8904, Japan (e-mail: teruyuki@ccsr.u-tokyo.ac.jp)

A. Higurashi, National Institute for Environmental Studies, Onogawa, Tsukuba, Ibaraki, 305-0053, Japan (e-mail: 16-2 hakiko@nies.go.jp)

K. Kawamoto, NASA Langley Research Center, Atmospheric Sciences Division, Mail Stop 420 Hamptom, VA 23681 (e-mail: k.kawamoto@larc.nasa.gov)

J. E. Penner, Department of Atmosphere, Oceanic and Space Sciences, University of Michigan, 2455 Hayward, Ann Arbor, MI 48109-2143 (e-mail: Penner@umich.edu)

(Received August 9, 2000; accepted November 30, 2000.)